

Optical fibers with interferometric path length stability by controlled heating for transmission of optical signals and as components in frequency standards

Holger Müller

*Physics Department, Stanford University, Stanford,
CA 94305. Fax: (650) 723-9173, Email: holgerm@stanford.edu.*

Achim Peters

*Institut für Physik, Humboldt-Universität zu Berlin, Hausvogteiplatz 5-7, 10117 Berlin,
Germany. Fax: +49 30 2093 4718, Email: achim.peters@physik.hu-berlin.de.*

Claus Braxmaier

*Hochschule für Technik, Wirtschaft & Gestaltung Konstanz, Brauneggerstr. 55,
78462 Konstanz. Fax: +49 (0)7531-206- 558, Email: braxm@fh-konstanz.de.*

We present a simple method to stabilize the optical path length of an optical fiber to an accuracy of about 1/100 of the laser wavelength. We study the dynamic response of the path length to modulation of an electrically conductive heater layer of the fiber. The path length is measured against the laser wavelength by use of the Pound-Drever-Hall method; negative feedback is applied via the heater. We apply the method in the context of a cryogenic resonator frequency standard.

PACS numbers: 42.81.Wg Other fiber-optical devices; 07.07.Mp Transducers; 07.07.Tw Servo and control equipment; robots.

I. INTRODUCTION

The transmission of light through optical fibers is ubiquitous in optics. However, fibers are easily deformed. Vibrations and temperature changes thus cause an unwanted modulation of the optical path length nL (where n is the index of refraction of the fiber core and L the mechanical length), thus phase modulating the transmitted signal. Even for fibers as short as a few meters under quiet laboratory conditions, the phase fluctuations easily exceed 2π on a timescale of seconds. When using fibers to transmit light between laboratories or different buildings, the corresponding broadening of the spectrum reaches several kHz [1]. At first glance, this may appear negligible against the frequency of optical radiation. However, the tremendous progress in optical frequency stabilization has lead to lasers with a linewidth of one Hz and below [2, 3, 4, 5, 6]. Such lasers are applied, for example, in optical clocks [7, 8] and tests of fundamental laws of physics [4]. Precision atomic physics experiments use phase-locked lasers having $\sim 10^{-8} \text{ rad}^2$ relative phase variance [9]. It is clear that transmission of such signals through fibers most significantly degrades their frequency and phase stability.

Path length fluctuations may also have considerable effects in other fields: For example, quantum cryptography bridges distances exceeding 100 km by fibers and is now beginning to be a commercial technology. Fiber length fluctuations are important in this context, since some concepts use interferometry to detect the quantum state of photons [10]. For global frequency comparisons at the targeted precision of next generation optical atomic clocks (10^{-18}), Doppler-shifts caused by the continental drift (at a velocity of $\sim 1 \text{ cm per year}$) will have to be

controlled. Moreover, fiber length fluctuations have been identified as a limit on the frequency noise of optical comb generators [11]. They also may play a role in space experiments like the LISA und LISA Pathfinder missions, which use Mach-Zehnder interferometers that have fibers in the interferometer arms. There is thus a strong and increasing need for a simple and reliable method to remove fiber path length fluctuations.

Cancellation of the phase errors caused by such fluctuations has been demonstrated by L.-S. Ma, P. Jungner, J. Ye, and J.L. Hall [1]. They use an acousto-optic modulator (AOM) to pre-modulate the fiber input with the negative image of the phase fluctuations, so that the fluctuations are cancelled at the fiber output. The fluctuations are measured by sending back a sample of the transmitted signal and comparing it to the incident one. This technique is applied in the operation, comparison and improvement of optical frequency standards [12], tests of fundamental physics [13], and may even be useful in quantum optics and atomic physics experiments, including quantum computing and cryptography [14].

In this paper, we describe the use of controlled heating of (a part of) the fiber for stabilizing or modulating the optical path length. It achieves a performance similar to that of the method reported by Ma *et al.*. We directly stabilize the path length itself rather than compensating for the phase modulation caused by the fluctuations. Our method does not require the use of an AOM. This simplifies the setup and avoids the loss of the optical power associated with the deflection efficiency of the AOM and makes our method useful even for signals, which cannot be transmitted through an AOM, such as the very broadband light found in optical comb generators.

This paper is organized as follows: In Sec. II we describe the dynamic response of the path length to the

heater. The setup and its performance are described in section III. In Sec. IV, we show how the method was used in an experiment on frequency stabilization in a fiber-coupled cryogenic optical resonator (CORE).

II. DYNAMIC RESPONSE OF THE FIBER

Thermal time constants can easily be of the order of minutes or longer. Thus, if heating is to be used as an actuator in a fast servo loop that achieves sub-wavelength stability, the dynamic response of the path length to heating has to be considered carefully. Previous studies of the static [15, 16] and the dynamic response [17, 18] assume that the fiber surface is heated to a fixed temperature by an external thermal source. However, for fast temperature changes, this assumption becomes unrealistic, since the finite thermal conductivity of any material precludes the instantaneous application of a fixed temperature. Rather, the dynamic characteristics of the thermal source itself have to be taken into account. We discuss the magnitude and the phase of the response, the latter being of prime interest for the design of a servo loop.

In our model, the response of the path length nL is given by changes in the index of refraction n and the physical length L of the fiber core:

$$\frac{\Delta(nL)}{nL} = \frac{\Delta n}{n} + \frac{\Delta L}{L} = \frac{1}{n} \beta \Delta T(0) + \frac{\Delta L}{L}, \quad (1)$$

where β is the thermooptic coefficient and $\Delta T(0)$ denotes the temperature change of the fiber core. The simplest model of the fiber is that of a homogenous solid cylinder. The propagation of heat is governed by the diffusion equation

$$\dot{T} = \bar{\lambda} \Delta T + H, \quad (2)$$

where $H(r, t)$ represents a heater which deposits an equal amount of thermal power into every volume element. $\bar{\lambda} = \lambda/(\rho c)$ is the thermal diffusion constant, given by the thermal conductivity λ , the mass density ρ , and the specific heat c . We first solve the homogenous equation with $H = 0$. In cylindrical coordinates r, φ, z , specializing to the relevant case of no dependence on φ and z ,

$$\dot{T} = \bar{\lambda} \left(\frac{1}{r} \frac{\partial}{\partial r} + \frac{\partial^2}{\partial r^2} \right) T. \quad (3)$$

We separate $T(r, t) \equiv \mathcal{T}(t)\mathcal{R}(r)$ and obtain a radial and a temporal differential equation

$$\mathcal{R}'' + \frac{1}{r} \mathcal{R}' - \frac{i\omega}{\bar{\lambda}} \mathcal{R} = 0, \quad \mathcal{T}' - i\omega \mathcal{T} = 0. \quad (4)$$

The separation constant is denoted $i\omega$. A solution to the temporal equation is proportional to $e^{i\omega t}$. The general solution to the radial equation can be written as

$$\mathcal{R} = A J_0(\sqrt{i\omega/\bar{\lambda}} r) + B N_0(\sqrt{i\omega/\bar{\lambda}} r). \quad (5)$$

TABLE I: Properties of fibers. See Tab. II for material properties.

	Plastic-jacketed	Aluminum-jacketed	Bare, gold-coated
Layer 1	Quartz glass	Quartz glass	Quartz glass
Layer 2	Acryl		
Layer 3	Conductive varnish	Aluminum	Gold
r_1 [μm]	60	60	60
r_2 [μm]	250		
r_3 [μm]	400	250	70

TABLE II: Material properties.

	Acryl	Quartz glass	Al	Conductive varnish	Au
λ [J/(K m s)]	0.19	1.36	220	20	312
ρ [kg/m ³]	2000	2200	2702	$\sim 10^4$	19290
E [GPa]	3	75	71	$\sim .005$	78
c [J/(kg K)]	1700	729	896	~ 400	129
α [10 ⁻⁶ /K]	80	0.45	23.8	~ 100	14.3
β [10 ⁻⁶ /K]		9			

J_0 and N_0 are the Bessel and Neumann functions of zeroth order and A and B are linear coefficients. For the innermost layer of the fiber, the B coefficient is required to vanishes since the Neumann function diverges for $r \rightarrow 0$.

Our model of the fiber consists of up to three concentric cylindrical layers (see Tables I and II): (i) the inner layer (radius r_1) represents both the fiber core and cladding. Although they are doped to obtain slightly different index of refraction, the thermal and mechanical properties of the two are alike, so in the thermal model they can be considered as a single layer. (ii) A protective jacket of outer radius r_2 , and (iii) a heater coating of outer radius r_3 . (For the gold and aluminum coated fibers, the coating itself acts as the heater; therefore, $r_1 = r_2$ and there are only two layers in the models for these fibers.) The linear coefficients A_i and B_i and the material parameters (Tab. II) for each layer are denoted by subscripts i that take the values 1,2,3. They are fixed by the boundary conditions that the temperature and the heat flow be smooth.

Within the heater volume, we assume a thermal source that is periodic in time:

$$H = \frac{h}{\rho c} e^{i\omega t}, \quad (6)$$

where h represents the power density of the heater in W/m³. The solution of the inhomogenous differential equation is the sum of a particular solution and the general solution of the homogenous equation. A particular solution

$$T(r, t) = \frac{h}{i\omega \rho c} e^{i\omega t} \quad (7)$$

can easily be found. We introduce the short notation

$$Z_n(i, j) \equiv Z_n \left(\sqrt{\frac{i\omega}{\lambda_i}} r_j \right), \quad (8)$$

where Z_n denotes any of the functions J_n and N_n . The boundary conditions are explicitly

$$\begin{aligned} A_1 J_0(1, 1) &= A_2 J_0(2, 1) + B_2 N_0(2, 1), \\ A_1 J'_0(1, 1) &= (\lambda_2/\lambda_1)[A_2 J'_0(2, 1) \\ &\quad + B_2 N'_0(2, 1)], \\ A_2 J_0(2, 2) + B_2 N_0(2, 2) &= A_3 J_0(3, 2) + B_3 N_0(3, 2) \\ &\quad + \frac{h}{i\omega \rho_3 c_3} e^{i\omega t}, \\ A_2 J'_0(2, 2) + B_2 N'_0(2, 2) &= (\lambda_3/\lambda_2)[A_3 J'_0(3, 2) \\ &\quad + B_3 N'_0(3, 2)], \\ A_3 J'_0(3, 3) + B_3 N'_0(3, 3) &= 0. \end{aligned} \quad (9)$$

The last equation means that for now we assume no heat dissipation to the environment, the effects of which will be discussed later. This system of linear algebraic equations can be solved for the coefficients A_i, B_i . Since the solution is elementary but lengthy, we will not spell it out here. The temperature of the core and thus the associated path length change $\beta\Delta T(0)$ are given by $\Delta T(0) = A_1 J_0(1, 1)$.

The additional strain term is caused by thermal expansion, which leads to axial strain (i.e., length change) [17, 18]. This changes the path length nL directly. (The temperature changes also cause radial strain which leads to a change in the phase velocity of light in the waveguide [17, 18]. However, as this effect contributes only about 10% of the total effect, we can neglect it here.) Each infinitesimal layer of the fiber wants to adjust its length according to the local temperature. For alternating temperatures, the temperature distribution is inhomogenous; stress builds up, which propagates to other layers at the speed of sound. For the time-scales relevant here, we can assume instantaneous sound propagation. Hence, the length of the fiber is then given by a balance of forces

$$\int r\alpha(r)E(r)T(r)dr = \Delta L \int r\lambda(r)dr. \quad (10)$$

Here, α is the thermal expansion coefficient and E the bulk modulus. These quantities appear under the integrals, because they are different for the layers of the fiber. Hence,

$$\Delta L = \frac{\int \alpha(r)\lambda(r)T(r)rdr}{\int r\lambda(r)dr}. \quad (11)$$

Using $\int xZ_0(x)dx = xZ_1(x)$ and defining $r_0 \equiv 0$,

$$\begin{aligned} \Delta L(\omega) &= \left(2 \sum_{k=1}^3 E_k (r_k - r_{k-1})^2 \right)^{-1} \\ &\quad \times \left(\frac{2\pi h}{i\omega \rho_3 c_3} \frac{r_3^2 - r_2^2}{2} + \sum_{k=1}^3 \frac{E_k \alpha_k \sqrt{\lambda_k}}{\sqrt{i\omega}} \right. \\ &\quad \left. \times \left[A_k r J_1 \left(\sqrt{\frac{i\omega}{\lambda_k}} r \right) + B_k r N_1 \left(\sqrt{\frac{i\omega}{\lambda_k}} r \right) \right]_{r_{k-1}}^{r_k} \right). \end{aligned} \quad (12)$$

The core temperature and the strain term have the same sign for slow temperature variations. In what follows, we study the path length change as given by these terms for the fibers listed in Tab. I.

a. Plastic-jacketed fiber The core temperature and the strain term for this fiber is shown in Fig. 1 (left). For better presentation in the figure, the amplitudes have been multiplied by the frequency f .

For frequencies below about 1 Hz, the amplitudes of the core temperature and the strain term are proportional to $1/f$; their phases equal -90° . This is because we neglect heat dissipation to the environment, which means that the actual thermal energy within the fiber is the integral of the heating rate over time. In practice, this is a good approximation for frequencies above about 0.1 Hz. At lower frequencies, the temperature of the fiber will be given by an equilibrium between heating and dissipation. Thus, the frequency response of the strain and core temperature terms will become constant below about 0.1 Hz. The phase will then be 0° . It is, of course, possible to incorporate dissipation into the above model. However, the heat dissipation is hard to quantify because of air currents. Moreover, it is irrelevant for the design of the fiber length feedback loop as it has significant effects only for frequencies much below the loop bandwidth.

For frequencies above about 0.5 Hz, the magnitude of both terms begins to drop, and the phase lags increase correspondingly. For the core temperature term, this is because fast temperature changes are attenuated on their way to the core due to the finite thermal conductivity. The core temperature term drops rapidly with increasing frequency and gains a large phase shift, which exceeds 180° for frequencies as low as 1 Hz. This bandwidth is much too low for an effective removal of the path length fluctuations by a servo loop.

Study of the strain term ΔL , however, reveals a much more favourable behaviour. Like the core temperature term, it starts to drop for frequencies above about 0.5 Hz, but only very mildly, proportional to $1/f^{3/2}$. This because the strain term does not depend on the slow heat diffusion to the core alone. Rather, strain generated in the outer layers of the fiber, which are closer to the heater, is transmitted to the core at the velocity of sound. The $1/\sqrt{f}$ roll off (in addition to the overall $1/f$ one) arises because the depth to which the temperature changes penetrate the fiber becomes thinner with increasing frequency. This mild frequency response is crucial for

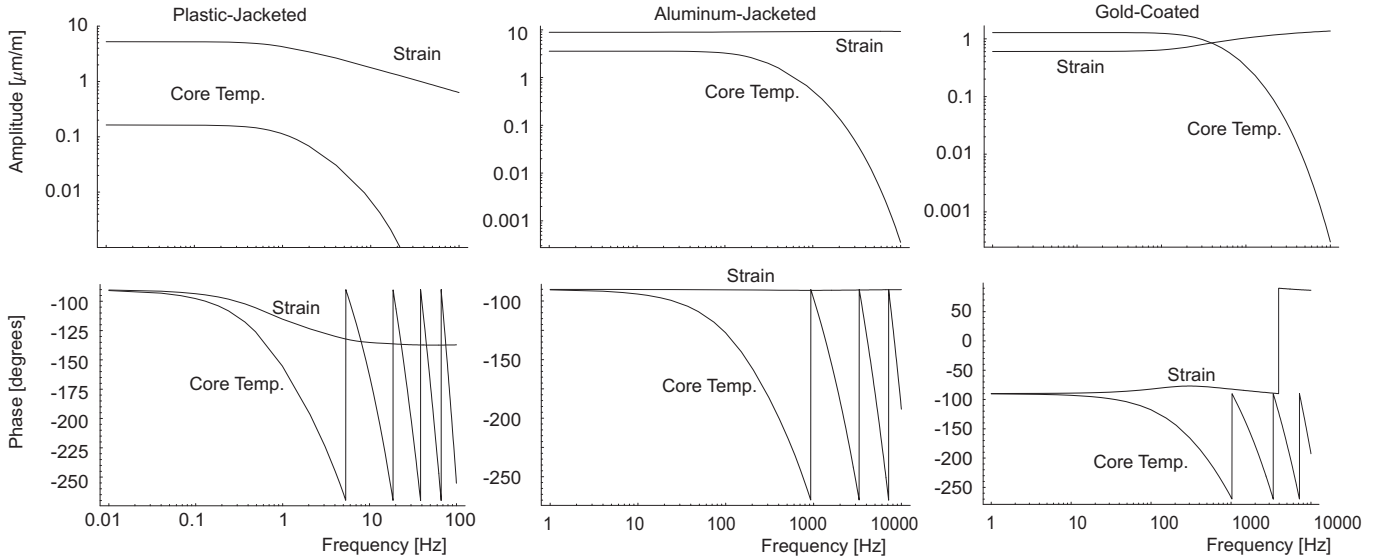


FIG. 1: Bode plots. Amplitude responses have been multiplied by the frequency f . We assume $h = 2\pi \text{ W/mm}^3$ heating power density (corresponding to 1.9, 1.1, and 0.25 W, respectively, per meter of fiber length).

the performance of the servo: The $1/f^{3/2}$ roll off at 135° total phase shift enables a fast and stable servo loop.

The actual frequency dependence of the strain term shown in Fig. 1 (left) is a consequence of the very low elastic modulus of the heater coating. A heater out of a more rigid material will cause a different, and even more interesting, response. This is made evident in the case of aluminum coated fiber, see below.

b. Aluminum-coated fiber Aluminum coated fiber, where the Al coating is used as the heater, has a frequency response which is even more suitable for the present application, see Fig. 1 (middle). Apart from a general $1/f$ response, the core temperature term begins to roll-off at a frequency of $f_1 \sim 250 \text{ Hz}$, much larger than for plastic jacket. This is because of the much larger thermal conductivity of the Al coating as compared to acryl, and because the Al coating as a heater attaches directly to the core.

The frequency response is again dominated by the strain term. The major difference to the plastic-jacketed fiber is that the strain term shows virtually no roll-off other than the usual $1/f$ behaviour for all frequencies at which the model is valid. This is because the Al coating as a high elastic modulus, comparable to the one of the quartz glass core. As the Al layer is much thicker than the core, the stiffness of the fiber is almost completely due to the Al heater layer. Heat is generated throughout the volume of the Al coating, and there it causes strain instantaneously. This strain is propagated to the core at the high velocity of sound.

c. Bare, gold-coated fiber The frequency response of fiber coated with a thin layer of gold is shown in Fig. 1 (right). The gold coating is used as the heater. The strain term is not dominant at low frequencies (because the stiffness of the fiber is dominated by the quartz glass core,

with its low thermal expansion coefficient), but overtakes for larger frequencies. The magnitude of the strain term depicts a roll-off of slightly less than $1/f$ for frequencies between 100 and 10000 Hz. The reason can be explained as follows: The thermal expansion coefficient of quartz glass is much lower than that of gold. Most stress is thus generated in the thin gold coating, and the resulting strain is reduced by the core due to its low thermal expansion coefficient. At low frequencies, the core also takes away a significant fraction of the thermal energy, thus reducing the amplitude of the temperature in the heater volume, thereby reducing the generated stress. At high frequencies, however, the finite thermal conductivity reduces the heat transfer to the core, so that the temperature variation is no longer reduced by heat transfer.

d. Discussion The phase modulation depth that can be achieved by heating is limited by the permissible temperature and hence the power dissipation of the heater. Assuming a very moderate heater power of 1 W per meter of fiber length, we obtain a modulation depth of about $2.4 \mu\text{m}/\text{m}$, $8 \mu\text{m}/\text{m}$, and $4 \mu\text{m}/\text{m}$ for plastic-, aluminum-, and gold-coated fiber at 1 Hz, respectively. The higher values are obtained for the aluminum- and gold-coated fibers, where this figure drops like $1/f$ (For the plastic-jacketed fiber, it drops with $1/f^{3/2}$).

The validity of the above model is limited at higher frequencies, since we assumed instantaneous sound propagation. Sound, however, propagates at a velocity of several 1000 m/s. For a fiber radius of $400 \mu\text{m}$, this means that fiber will deviate from the above model on a time scale of the order of $0.1 \mu\text{s}$, or frequencies of a few MHz. Since the additional delay due to the finite velocity will increase the phase lag at high frequencies, this represents a theoretical limit on the speed of any feedback loop based on heating of a fiber. In view of the very limited modulation

amplitude that can be reached at such high frequencies, however, heating of the fiber cannot take out a disturbance of any appreciable amplitude at such frequencies, even if the linearized feedback loop would theoretically be stable.

III. APPARATUS

A. Overview

The basic setup is shown in figure 2. For reading out the instantaneous length of the fiber, we use the method developed by Pound, Drever, and Hall [19] for reading out the resonance frequency of a resonant cavity. Indeed, the fiber with its about 4% parasitic reflection at each end resembles a Fabry-Perot etalon, although one with a quite low finesse. A frequency modulated Nd:YAG laser light at 1064 nm is sent through the fiber. The modulation frequency is $f_m = 500$ kHz with a modulation index of about 1 (however, these parameters are not critical for the performance of the active length control). From the output of the fiber, we split off a sample and detect its intensity. Alternatively, the detector can be placed at the input of the fiber. This makes the setup extremely simple, as no additional components are required at the remote end of the fiber.

Due to the frequency modulation (FM), the laser radiation acquires additional Fourier components at frequencies $f_l \pm f_m$ (“sidebands”), where f_l is the laser frequency. For pure FM, the phase relationship between these components is such that the amplitude of the signal is unaffected. The resonant and dispersive properties of the fiber alter these phase relationships. In general, this converts the pure frequency modulation into amplitude modulation (AM) components at multiples of ω_m . When the laser and the resonance frequency coincide, the detected component of the AM vanishes; if they are detuned, however, a nonzero AM is found, whose amplitude indicates the magnitude and whose phase relative to the FM indicates the direction of the detuning. The detector signal is multiplied with a local oscillator (LO) signal at f_m in a double-balanced mixer (DBM), and the output of the DBM is low-pass filtered to suppress the modulation frequency. With the correct LO phase ϕ , a error signal is thus generated that indicates the deviation of the optical path length of the fiber relative to a multiple of half the laser wavelength.

This signal serves as input to a proportional-integral servo, which controls the fiber length by heating a part of the fiber. For determining the gain and time constants of the servo, we use the results of our above study of the dynamic response of the fiber (Fig. 1). Since a servo loop is stable for a $1/f^{3/2}$ roll off with a corresponding phase shift of 135 degrees, it can operate throughout the frequency range discussed in the above model.

The most suitable fiber would be the aluminum-jacketed or gold-coated ones (Tab. I). The most unde-

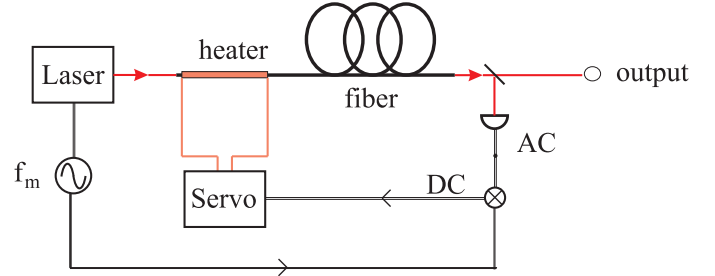


FIG. 2: Basic setup for active length control of an optical fiber: The frequency modulated laser light is sent through the fiber and detected by a photodetector. Demodulation with the modulation frequency yields an error signal, that is used by a servo to drive a heater in order to compensate for fluctuations in length. It is also possible to place the detector and beamsplitter to the input side of the fiber.

sirable one, from the point of view of high servo speed, is plastic-jacketed fiber, because the plastic jacket is thick and has poor thermal conductivity. The results of the previous section, however, show that even in this case loop bandwidths of several 100 Hz can be achieved.

To demonstrate that even in this case a satisfactory performance can be obtained, we used a 5 m long polarization maintaining fiber with plastic jacket (Thor labs type FS-PM-4511). We tried two different methods to attach a heater layer to it: A manganine wire wrapped around the fiber did not work because of the bad thermal contact between the wire and the fiber. Much better contact was obtained by coating the fiber with electrically conductive silver varnish on a length of 30 cm.

To examine the length stability of the fiber, we monitor the error signal with the servo loop open and closed, which yields a measurement of the actuator-limited performance of the servo loop (Errors in the fiber length sensing by the Pound-Drever-Hall method are not necessarily revealed in this measurement, but should be negligible here.) Without stabilization, the fluctuations reach up to $0.5\mu\text{m}/\sqrt{\text{Hz}}$ at 1 Hz and increase proportionally to $1/f^2$ for lower frequencies. Fig. 3 does only show this for frequencies above 1 Hz, because the length readout provided by the Pound-Drever-Hall method is restricted to a range of $\lambda/2$. Applying active length stabilization, the fluctuations are reduced below $8\text{ nm}/\sqrt{\text{Hz}}$ for frequencies below about 1 Hz, and below $1\text{ nm}/\sqrt{\text{Hz}}$ above 1 Hz. The fluctuations integrated over the frequency range of Fig. 3 are about 10 nm, or $\lambda/100$.

Given the simplicity of our setup, these results compare well to those due to Ma *et al.* [1]: For 25 m of fiber, within a frequency band of $\sim 0.01 - 2$ kHz, they suppressed the phase noise to a level of -60 dBc/Hz, corresponding to residual length fluctuations below $\sim 1\text{ nm}/\sqrt{\text{Hz}}$. The noise is increasing to $1\mu\text{m}/\sqrt{\text{Hz}}$ at 0.1 Hz, but this is a very conservative value, as Ma *et al.* infer it directly from a beat measurement between the incident and the transmitted light. Although the bandwidth of our lock

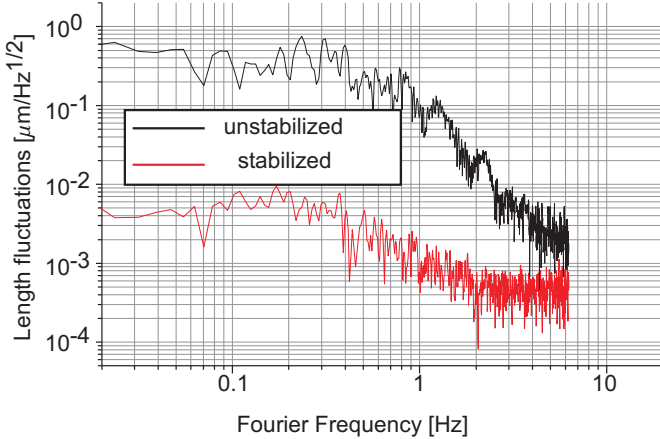


FIG. 3: Path length fluctuations with and without stabilization.

(~ 200 Hz) is lower than in the previous work, our setup achieves a similar performance for low and medium frequencies.

In many cases, the frequency modulation used for reading out the path length will not interfere with the intended application of the fiber's output signal. The sidebands form separate components in frequency space; in a frequency comparison by taking a beat note with another optical signal, for example, they can be removed by electronic filtering. Its effects can be reduced by using a low modulation index and by choosing a suitable modulation frequency.

The coating with silver varnish turned out to be unsuitable for a long term usage. Occasionally, it breaks at its weakest point, which makes further length controlling impossible. Although the defect can easily be repaired and the fiber itself does not suffer any damage, a reliable long-term performance requires a more stable solution, like using of aluminum-jacketed fiber (Tab. I).

IV. APPLICATION WITHIN A CRYOGENIC RESONATOR FREQUENCY STANDARD

We applied the method in an optical frequency standards based on a Nd:YAG laser stabilized to a cryogenic optical resonator (CORE), see figure 4. This consists of an oscillator, a monolithic, diode-pumped neodymium-YAG laser, frequency stabilized to a CORE located inside a liquid helium cryostat. The frequency stabilization uses the Pound-Drever-Hall method using a photodetector that detects the light that is reflected from the core (Fig., 4, above). In previous work, this system was shown to reach a Hz-level stability on a timescale of seconds.

An optical fiber is used for coupling the laser light to the cavity (Fig. 4). While this made the system more stable on timescales of hours [20, 21], on short timescales, however, the frequency stability with fiber coupling is reduced due to path length fluctuations. These introduce

phase fluctuations as described above, as they shift the laser frequency relative to the CORE resonance. Additionally, since the fiber with parasitic reflections at its ends acts like a Fabry-Perot etalon, it adds parasitic signal components into the Pound-Drever-Hall error signal used for feeding back to the laser frequency. These change from maximum to minimum for a $\lambda/4$ length change of the fiber and cause an unwanted fluctuation of the baseline of the error signal (Fig. 5 (above)), which have been found to lead to fluctuations of the Nd:YAG laser frequency of 8 Hz amplitude.

To remove both the Doppler effect and this modulation, we lock the path length of the fiber to the Nd:YAG laser's wavelength using the method described above: A photodetector located inside the cryostat (Fig. 4, below) is used to read out the fiber length fluctuations. Its signal is downconverted with the laser modulation frequency to generate an error signal for reading out the fiber length. It is fed back to the heater via a proportional-integral controller. The fiber and the heater are of the same type as described above.

Figure 5 illustrates the effect of fiber-length stabilization. Above is shown the error signal without active fiber length stabilization, measured by scanning the laser frequency over a range of about 150 MHz. Note the baseline fluctuations caused by the parasitic etalon due to the fiber with a free spectral range of about 50 MHz. Active fiber length control tracks the fiber length according to the actual laser wavelength and removes these effects (Fig. 5 (below)). For the 150 MHz laser frequency sweep, the fiber length changes by about $2.5 \mu\text{m}$ to track the fiber length to the actual laser wavelength. Thus, the fiber is always operated with maximum transmission, where the front and the back reflex cancel. A straight baseline free from the etalon fringes seen in Fig. 5 (above) and a constant signal amplitude at maximum value are obtained. The speed of the servo loop made it possible to track the laser wavelength even while it was scanned at a rate of about 10 Hz.

Additionally, the error signal used for stabilizing the laser frequency can be improved by introducing a fraction of the “fiber”-detector's signal into the path of the “CORE” detector. Adjusting the amplitude and phase relationships between the two carefully, an additional cancellation of the unwanted signal components due to the fiber can be achieved.

V. SUMMARY AND OUTLOOK

We have presented a method to reduce fluctuations of the optical path length of optical fibers to below 10 nm by controlled heating of part of the fiber. A theoretical study of the response of the optical path length to heat dissipated in the bulk of a heater layer indicates that servo bandwidths in the kHz range, or indeed even the low MHz range, can be obtained. The high speed is because strain propagates in the fiber at the speed of sound,

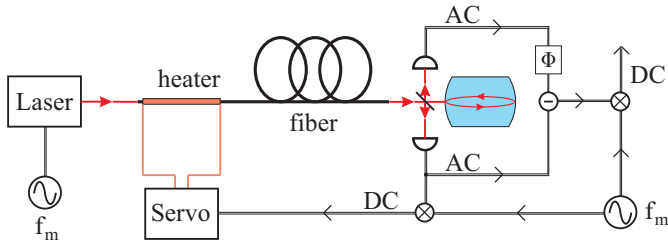


FIG. 4: Fiber length stabilization in a CORE frequency standard

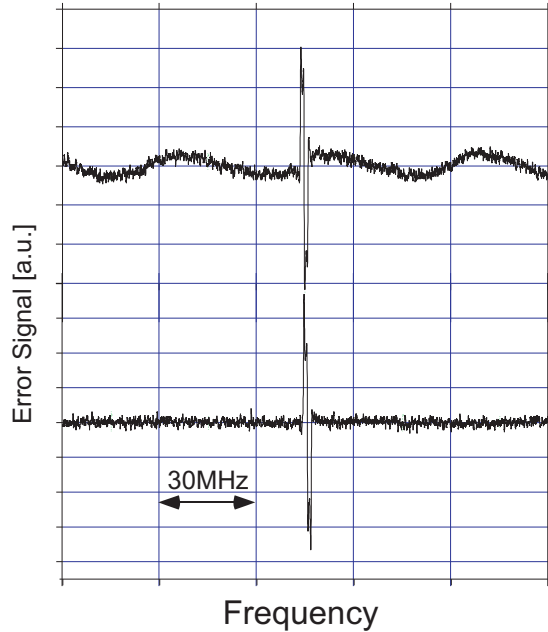


FIG. 5: Error signals without and with active fiber length stabilization.

which is a much faster process than heat diffusion. The most suitable fibers for this purpose are bare fiber with a thin gold coating for resistive heating, or aluminum jacketed one.

We also present a first experimental demonstration of the method. It uses a conductive coating made of silver varnish on a plastic-jacketed fiber. We used this method in the context of an optical frequency standard based on a cryogenic optical resonator.

Compared to previous work, our method has the advantage of simplicity. Moreover, since it directly removes the path length fluctuations, it can reduce the phase noise induced by such fluctuations for any signals, even those for which acousto-optic modulators are not suitable, like the broadband optical signals in optical frequency comb generators.

The simple realization of the presented idea for an active stabilization leaves plenty of space for further developments. Use of aluminum-jacketed fiber can enhance the reliability and also increases the useful lock bandwidth significantly. This leads to better stability of the stabilized path length. Another approach could be to try a bare fiber coated with a gold layer as a heater, which would lead to even better performance. We expect that the method can soon be routinely applied in many applications mentioned in the introduction, that require the transmission of an optical signal through fiber with exceptional stability.

VI. ACKNOWLEDGEMENTS

We thank Stephan Eggert for building excellent electronic circuits. H.M. wishes to thank S. Chu and S.-w. Chiow for discussions and the Alexander von Humboldt-Stiftung for support.

[1] L.-S. Ma, P. Jungner, J. Ye and J. L. Hall, Opt. Lett. **19**, 1777-1779 (1994).

[2] B. C. Young, F. C. Cruz, W. M. Itano, and J. C. Bergquist, Phys. Rev. Lett. **82**, 3799 (1999).

[3] A. Y. Nevsky, M. Eichenseer, J. von Zanthier, and H. Walther, Opt. Commun. **210**, 91 (2002).

[4] H. Müller *et al.*, Phys. Rev. Lett. **91**, 020401 (2003); Opt. Lett. **28**, 2186 (2003); Appl. Phys. B (laser opt.) **77**, 719 (2003).

[5] S. A. Webster, M. Oxborrow, and P. Gill, Opt. Lett. **29**, 1497 (2004).

[6] M. Notcutt, L.-S. Ma, J. Ye, and J.L. Hall, Opt. Lett. **30**, 1815 (2005).

[7] Th. Udem, R. Holzwarth, T. W. Hänsch, Nature (London) **416**, 233 (2002).

[8] G. Wilpers, T. Binnewies, C. Degenhardt, U. Sterr, J. Helmcke, F. Riehle, Phys. Rev. Lett. **89**, 230801 (2002).

[9] H. Müller, S.-w. Chiow, Q. Long, and S. Chu, physics/0507187; Opt. Lett., in press (2005).

[10] C. Gobby, Z.L. Yuan, and A.J. Shields, Appl. Phys. Lett. **84**, 3762-3764 (2004).

[11] K. Imai, Y. Zhao, M. Kourogi, B. Widjyatmoko, M. Ohtsu, Opt. Lett. **24**, 214-216 (1999).

[12] B. de Beauvoir, F. Nez, L. Hilico, L. Julien, F. Biraben, B. Cagnac, J.J. Zondy, D. Touahri, O. Acef, and A. Clairon, Eur. Phys. J. D **1**, 227 (1998).

[13] S. Bize, S.A. Diddams, U. Tanaka, C.E. Tanner, W.H. Oskay, R.E. Drullinger, T.E. Parker, T.P. Heavner, S.R. Jefferts, L. Hollberg, W.M. Itano, and J.C. Bergquist, Phys. Rev. Lett. **90**, 150802 (2003).

[14] F. Schmidt-Kaler, S. Gulde, M. Riebe, T. Deuschle, A. Kreuter, G. Lancaster, C. Becher, J. Eschner, H. Haffner, and R. Blatt, J. Phys. B **36**, 623 (2003).

[15] N. Lagakos, J.A. Bucaro, and J. Jarzynski, Appl. Opt. **20**, 2305 (1981).

[16] N. Shibata, K. Katsuyama, Y. Mitsunaga, M. Tateda, and S. Seikai, Appl. Opt. **22**, 979 (1983).

[17] R. Hughes and R. Priest, Appl. Opt. **19**, 1477 (1980).

- [18] L. Schuetz, J.H. Cole, J. Jarzynski, N. Lagakos, and J.A. Bucaro, *Appl. Opt.* **22** (1983).
- [19] R.W.P. Drever, J.L. Hall, F.V. Kowalski, J. Hough, G.M. Ford, A.J. Munley, and H. Ward, *Appl. Phys. B* **31**, 97 (1983).
- [20] C. Braxmaier, H. Müller, O. Pradl, J. Mlynek, A. Peters, and S. Schiller, *Phys. Rev. Lett.* **88**, 010401 (2002).
- [21] C. Braxmaier, O. Pradl, B. Eiermann, A. Peters, J. Mlynek, and S. Schiller, in *Proceedings of the Conference on Precision Electromagnetic Measurements, 2000* (IEEE Instrumentation and Measurement Society, 2000).